

---

## JET deuterium: tritium results and their implications

M. Keilhacker

*Phil. Trans. R. Soc. Lond. A* 1999 **357**, 415-442

doi: 10.1098/rsta.1999.0335

---

### Email alerting service

Receive free email alerts when new articles cite this article - sign up in the box at the top right-hand corner of the article or click [here](#)

---

To subscribe to *Phil. Trans. R. Soc. Lond. A* go to: <http://rsta.royalsocietypublishing.org/subscriptions>

---

# JET deuterium–tritium results and their implications

BY M. KEILHACKER

*JET Joint Undertaking, Abingdon, Oxfordshire OX14 3EA, UK*

During the second half of 1997, JET carried out a broad-based series of experiments in deuterium–tritium (D–T) producing a total of 675 MJ of fusion energy and setting records for fusion power (16 MW), ratio of fusion power to plasma input power (0.62, and  $0.95 \pm 0.17$  if a similar plasma could be obtained in steady state) and fusion duration (4 MW for 4 s). A large-scale tritium supply and processing plant, the first of its kind, allowed the repeated use of the 20 g of tritium on site, supplying a total of 99.3 g of tritium to the machine.

The D–T physics programme allowed the size, heating requirements and operating conditions of the International Thermonuclear Experimental Reactor (ITER) to be defined more precisely. The threshold power required to access the high confinement operating mode foreseen for ITER is significantly lower in D–T than in deuterium (giving increased operational flexibility for ITER), but the global energy confinement time itself is practically unchanged (no isotope effect). ITER demonstration pulses, in which the important dimensionless parameters for confinement were matched to those of ITER, predict ignition for ITER provided the required densities can be reached. Three radiofrequency schemes for heating ITER were also tested successfully in D–T. The results agreed well with code calculations, giving confidence in the use of these models for predicting ICRF heating in future machines. Finally, the D–T experiments provided the first clear evidence of  $\alpha$ -particle heating, showing it to be consistent with classical expectations and confirming the process by which ignition and thermonuclear burn will occur in ITER and a fusion reactor.

**Keywords:** magnetic confinement fusion; deuterium–tritium experiments; fusion performance; ITER predictions;  $\alpha$ -particle heating; tritium retention

## 1. Introduction

The Joint European Torus (JET) is the only tokamak experiment that was designed from the outset for deuterium–tritium (D–T) operation and uses comprehensive tritium processing and remote handling systems. In 1991, after eight years of operation, JET had achieved a plasma performance in deuterium, which, if reproduced in a 50:50 D:T mixture, would have constituted breakeven conditions. It was decided that this performance warranted a ‘preliminary tritium experiment’ (PTE) to gain experience with D–T mixtures and to validate D–T fusion predictions. To limit the activation of the machine, a mixture of only 10% tritium and 90% deuterium was used and only two, practically identical, pulses were carried out. Each pulse produced a peak fusion power of 1.7 MW averaging 1 MW for 2 s and a fusion gain  $P_{\text{fus}}/P_{\text{in}} = 0.12$  (JET Team 1992). This was the world’s first controlled production of significant fusion power.

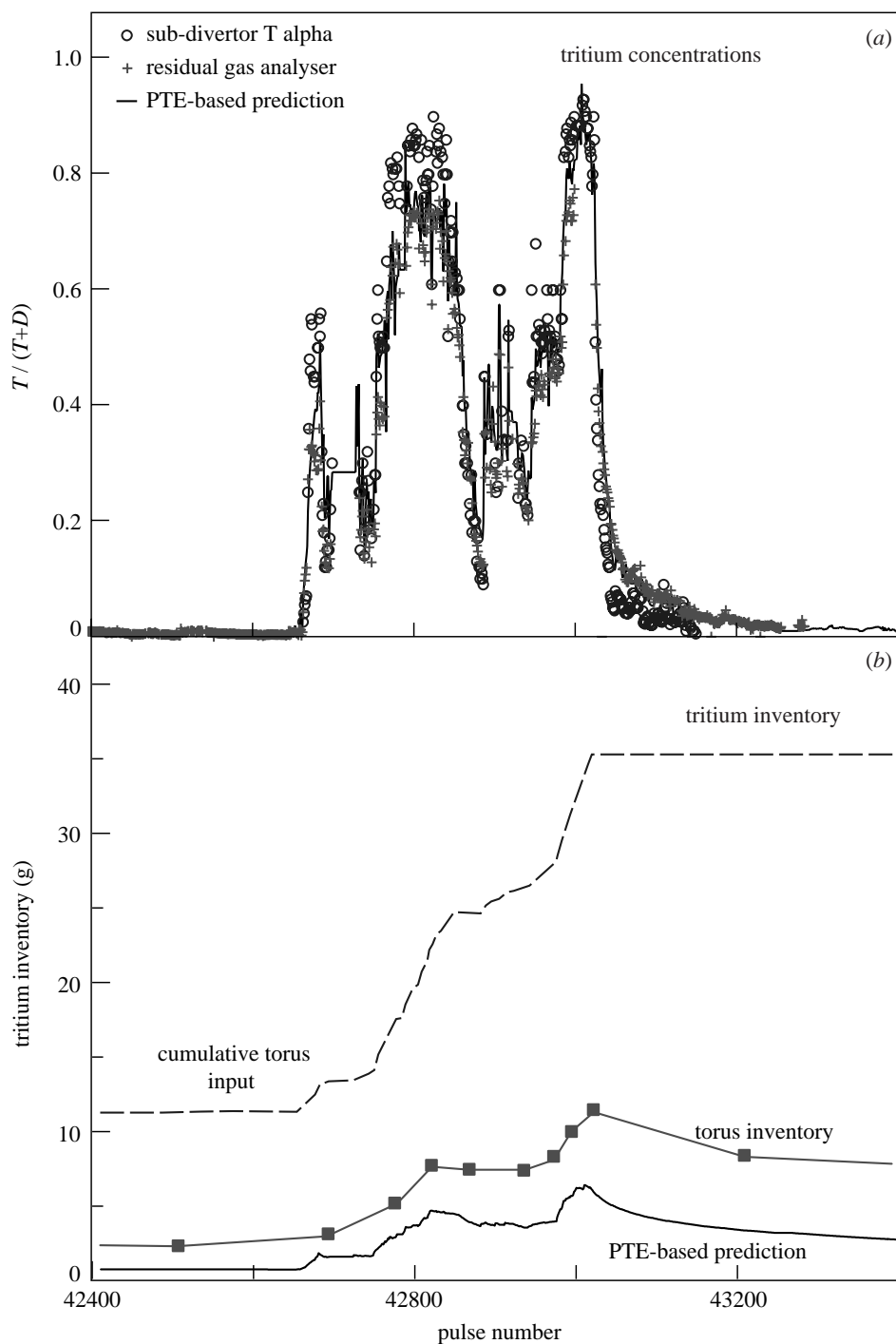


Figure 1. (a) Tritium concentrations and (b) tritium inventory in JET for the period September–November 1997 (the D–T experiments comprised pulses no. 42 661–43 023).

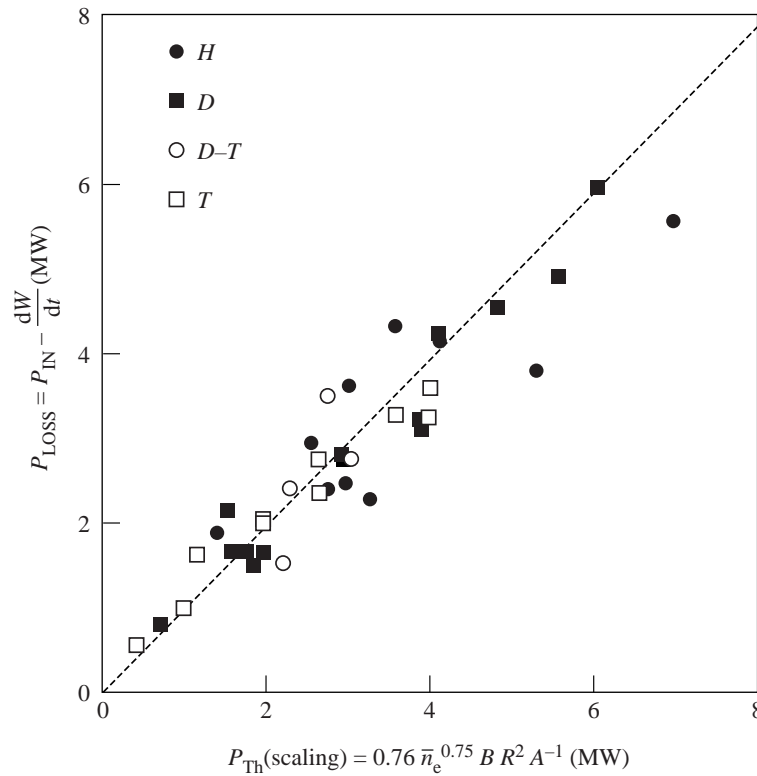


Figure 2. Plasma loss power for ELMy H-mode discharges in hydrogen, deuterium, deuterium–tritium and tritium plotted against the ITER scaling for the H-mode threshold power modified to include an inverse mass dependence.

In 1997 (May–June and September–November), JET resumed D–T operation with a broad-based but closely focused series of D–T experiments (DTE1) that addressed specific questions relating to D–T physics and technology for the International Thermonuclear Experimental Reactor (ITER) and a reactor. This paper describes the results from these D–T experiments (see also Gibson *et al.* 1998; Keilhacker *et al.* 1999; Jacquinot *et al.* 1999), and discusses their implications for the approach to ignition in general, and, more specifically, for the extrapolation to ITER (Aymar *et al.* 1997), defined as the plasma core of a future fusion reactor, i.e. demonstrating ignition and long pulse burn.

JET is unique for providing pertinent results in this area. It is essentially a one-third scale model of ITER, nearest in size and operating conditions to ITER and with a very similar plasma and divertor configuration. In addition, after the completion of TFTR in April 1997, JET is now the only experiment worldwide that is able to operate with D–T mixtures. JET has also developed a unique capability for remote installation and repair, which was used successfully earlier in 1998 for a major modification to its divertor in the activated environment following DTE1.

In the context of the approach to an ignited plasma, the paper addresses four major issues of fusion physics. The first is to define the parameters of a ‘next step’ tokamak and the JET results confirm that the ITER parameters are the right ones for its

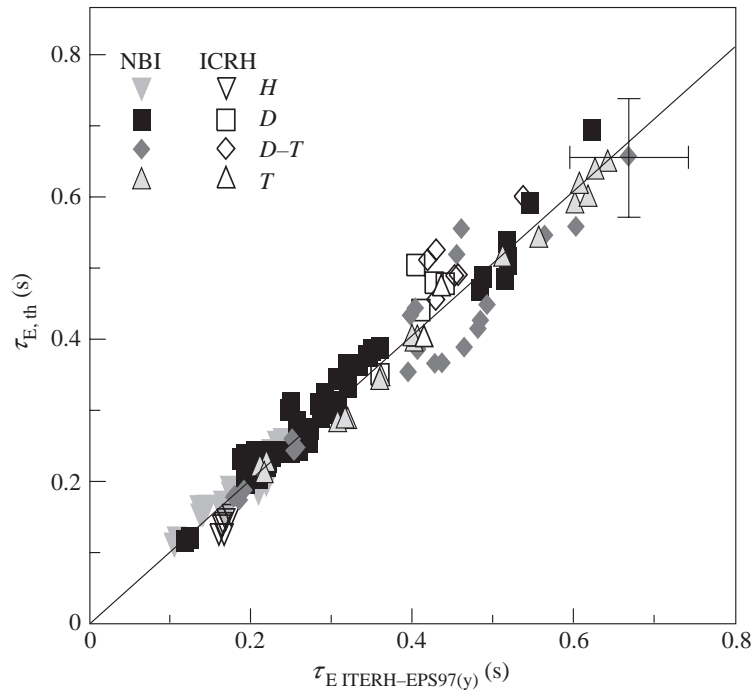


Figure 3. Measured thermal energy confinement times in hydrogen, deuterium, deuterium–tritium and tritium ELMy H-mode discharges plotted against the ITER scaling law.

stated objectives. The second issue is to characterize the standard operating mode for ITER, the ELMy H-mode. Here, the JET D–T results allow a more accurate assessment of the ignition margins and heating requirements of ITER. The third issue is to confirm the process by which ignition and burn would occur in ITER and a reactor. The JET results help to validate the high-performance physics in D–T and, in particular, provide an unambiguous demonstration of  $\alpha$ -particle heating. The fourth issue addressed is the optimization of tokamak operation for ignition and long pulse operation at reduced plasma current (and thereby size and cost) in ITER and a reactor. Here, the JET experiments provide the first demonstration in D–T of the control of plasma profiles in such an advanced operating mode, the so-called optimized-shear scenario. This discussion of fusion physics issues is complemented by a section on tritium retention where JET has gained valuable information for ITER.

The paper is structured in the following way. Section 2 discusses how the tritium was supplied to the torus and how much remained in the torus after DTE1. Section 3 characterizes the standard operating mode for ITER (steady-state ELMy H-mode) in D–T, addressing the isotope effect on both the threshold power for high confinement and the energy confinement time itself, and predictions to ITER. Section 4 deals with ion cyclotron resonance frequency heating of ELMy H-mode D–T plasmas. Section 5 addresses D–T performance and related physics, including records in fusion performance, Alfvénic instabilities and  $\alpha$ -particle confinement and heating. Section 6 presents the advanced operating mode for ITER (optimized-shear mode) in D–T: the formation of an internal transport barrier (ITB) with diffusion coefficients reduced to neoclassical values, the coexistence of internal and edge transport barriers and

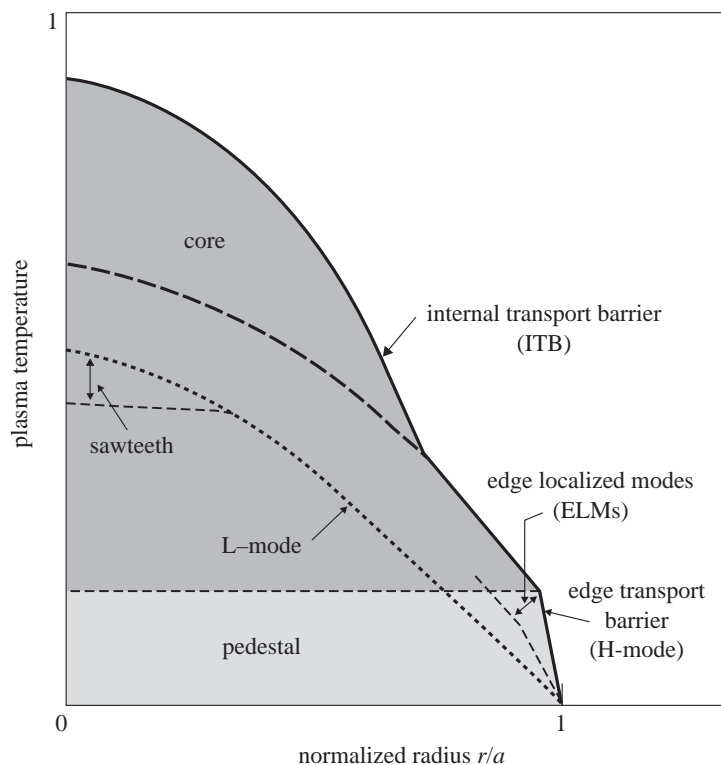


Figure 4. Characteristic plasma temperature profiles in different modes of tokamak operation: L-mode; H-mode with edge transport barrier; and optimized shear mode with ITB.

the possible development of this scenario towards steady state. The summary and conclusions follow in § 7.

## 2. Tritium supply, concentrations and inventory

During DTE1, 20 g of tritium were stored on the JET site in U-beds. This tritium was supplied, collected from the exhaust gases and reprocessed by an industrial-scale tritium-processing plant that worked in a closed cycle with the tokamak, pumping the torus in continuous operation. In all, 99.3 g of tritium was supplied to the JET machine, requiring eight processing cycles in which the tritium was routinely separated to better than 99.5% purity. The tritium gas was either injected directly into the torus via a gas valve (a total of 35 g) or by ‘neutral-beam’ (NB) injection. In this latter case, only a small fraction of the tritium gas supplied to the NB box was injected into the torus via the high-energy tritium neutral beams. The remaining tritium gas was trapped by the NB cryopumps and was recovered to better than 98% in nightly regenerations.

One of the experiences of DTE1 was that the tritium concentrations in the plasma could be relatively easily controlled by loading the walls to an appropriate level of tritium using ohmic or low-power ICRF heated discharges. As shown in figure 1*a*, plasma tritium concentrations greater than 90% were readily obtained. Figure 1*a* also shows that during DTE1 and the ensuing clean-up phase, tritium concentrations in

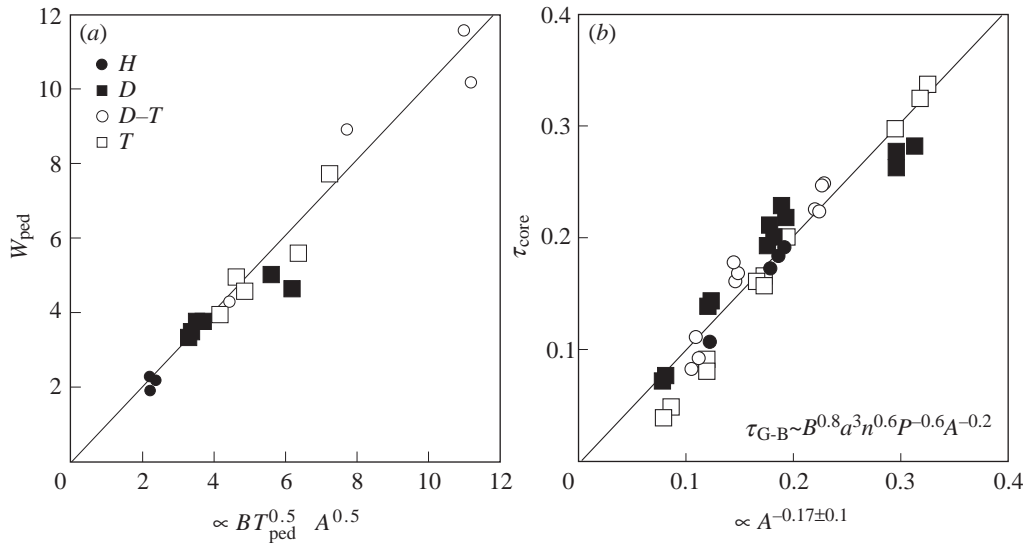


Figure 5. (a) Pedestal energy plotted against that expected from an edge-pressure gradient limited by ballooning modes over an ion poloidal Larmor radius; and (b) the thermal confinement time of the core plasma plotted against the best fit for the mass dependence in a pure gyro-Bohm scaling for ELMy H-mode discharges in hydrogen, deuterium, deuterium–tritium and tritium.

the plasma and exhaust gases were reduced at a rate similar to the experience from the PTE (Andrew *et al.* 1999).

In contrast, the tritium inventory (figure 1b) developed quite differently to the experience from the PTE: during the DTE1 campaign, about 30% of the cumulative tritium input remained in the torus. This level was reduced to about 17% (*ca.* 6 g) following extensive operation in hydrogen and deuterium; this was more than three times larger than had been expected from the tritium-retention results of the PTE. This high level of tritium retention during and after DTE1 has been related to carbon films, saturated with deuterium and tritium and found in cold regions of the divertor (Andrew *et al.* 1999). While most of the JET vessel was heated to 320 °C, these cold regions, shadowed from direct contact with the plasma, were cooled to *ca.* 50 °C (they act as a heat shield to protect the in-vessel divertor coils), allowing stable films to form with more than 40% hydrogen concentrations in carbon. (In contrast, at the time of the PTE, i.e. before the installation of a divertor, the whole vessel was maintained at 300 °C.) Extrapolation of these tritium retention results to ITER would result in unacceptably high tritium inventories, and the ITER divertor needs to be redesigned to take this fully into account.

### 3. Standard operating mode for ITER: steady-state ELMy H-mode in D–T

#### (a) Mass scaling of H-mode threshold power

The effect of isotope mass on the heating power needed to access the H-mode regime (the H-mode threshold power) was studied during DTE1 in a series of experiments which included discharges with *ca.* 60% and *ca.* 90% tritium concentrations in deu-

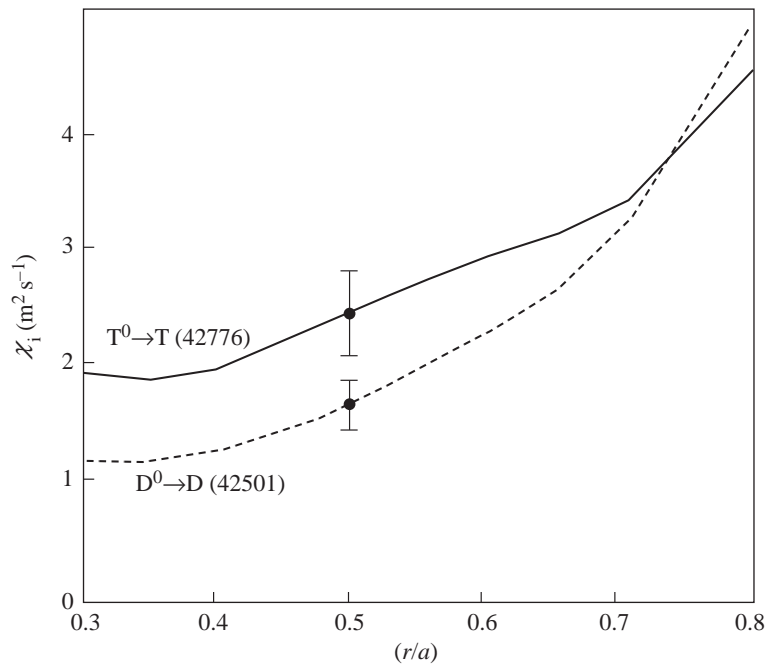


Figure 6. Ion thermal diffusivities versus normalized plasma radius for ELMy H-mode discharges in deuterium and tritium.

terium. The most notable result was that, in comparison with previous experiments in pure deuterium, the H-mode threshold power was lower in D–T and lower still in pure tritium, roughly as the inverse of the atomic mass ( $A^{-1}$ ). This can be seen in figure 2, which shows the loss power from the plasma plotted as a function of the scaling

$$P_{\text{th}} = 0.76 \bar{n}_e^{0.75} B R^2 A^{-1},$$

which has been modified from that used for ITER (ITER 1997a) by the inclusion of an inverse mass dependence (the constant of proportionality has been adjusted to give the best fit to these JET data). Following DTE1, similar experiments were carried out in hydrogen and these data are also shown in figure 2 and confirm the strong inverse mass dependence.

This result is very favourable for ITER since it predicts a 33% reduction in the power needed to access the H-mode in a pure tritium plasma (for example, during the start-up phase when it is important to achieve the high confinement of the H-mode as early as possible), and a 20% reduction in the H-mode threshold power for a 50:50 mixture of deuterium and tritium, thereby increasing the operational flexibility of ITER.

#### (b) Mass dependence of energy confinement in ELMy H-modes

The most recent version of the multi-machine database for steady-state ELMy H-mode discharges shows that the global energy confinement timescales as  $A^{0.2}$  with mass (the ITERH-EPS97(y) scaling (ITER 1997b), which is used at present



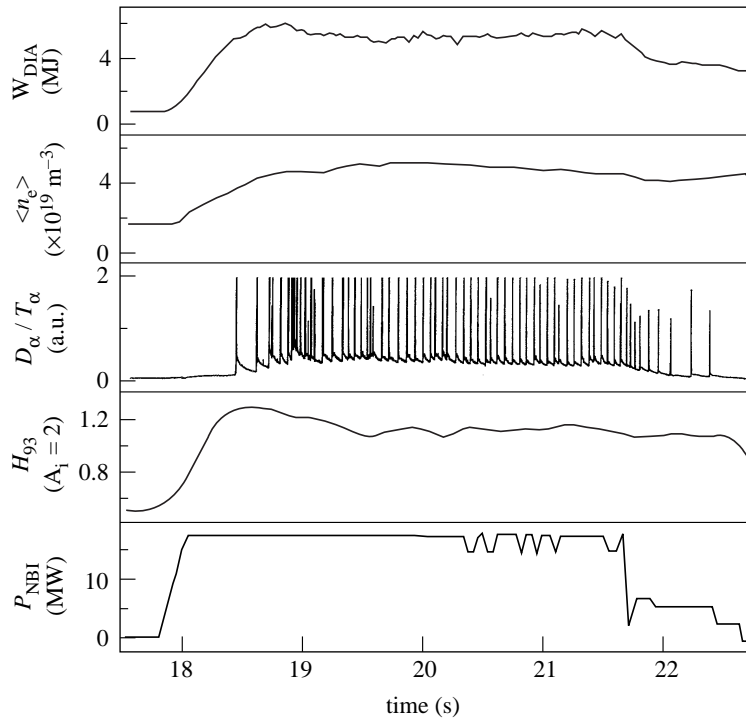


Figure 7. Steady-state ELMy H-mode with ITER collisionality and normalized plasma pressure ( $\beta_N = 2.4$ ) in D–T. Basis for ‘wind tunnel’ experiments in JET. Pulse no. 42756; 2 MA/2 T.

for extrapolation to ITER). Before, during and after DTE1, steady-state ELMy H-modes were obtained for a wide range of plasma currents (1–4.5 MA) and toroidal fields (1–3.8 T) in hydrogen, deuterium, D–T and tritium. The energy confinement times in these discharges were found to be consistent with the ITERH-EPS97(y) scaling, with its  $A^{0.2}$  dependence providing an acceptable fit (figure 3). However, a more refined analysis shows that a better fit is with practically no mass dependence ( $A^{0.03 \pm 0.1}$ ).

This result presents a challenge to theoretical understanding that may be resolved by separating the total stored plasma energy into two components (figure 4) that scale differently with respect to mass (and other significant parameters). The first component is the pedestal energy (figure 5a), which is determined from the edge temperature and density (assuming equal electron and ion temperatures at the plasma edge), and which shows a strong mass dependence. The data shown are fitted by an  $A^{0.5}$  dependence that would result, for example, from the gradient of the plasma pressure being limited in the edge by ideal ballooning-mode instabilities over a distance characterized by the Larmor radius of ions (JET Team 1997a). The second component is the core energy, which is determined by subtracting the pedestal energy from the total thermal plasma energy. The corresponding thermal core-energy confinement time

$$\tau_{\text{th,core}} = (W_{\text{th}} - W_{\text{ped}})/P$$

(figure 5b), is found to scale as  $A^{-0.17 \pm 0.1}$ , consistent with the  $A^{-0.2}$  mass dependence

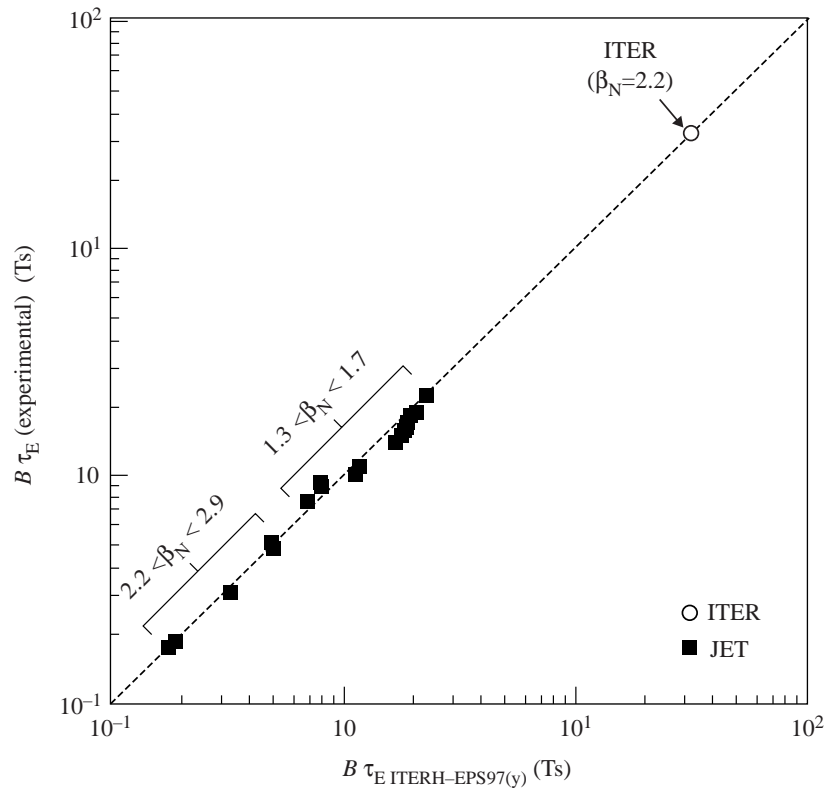


Figure 8. Measured thermal-energy confinement times of ITER similarity ELMy H-mode discharges in D–T plotted against the scaling law used in ITER projections. The operating point of an ignited ITER is also shown.

that would be expected from a gyro-Bohm scaling, generic of theoretical transport models based on turbulence with a scale length of the ion Larmor radius.

Differences between the edge and core transport are confirmed by local transport analysis using the TRANSP code. Figure 6 shows the ion thermal diffusivities as a function of normalized plasma radius for similar discharges in pure deuterium and in a 50:50 D–T mixture. It is clear from the figure that the mass dependence is different in the plasma core and edge, with the core data being consistent with the gyro-Bohm scaling ( $A^{0.5}T^{3/2}B^{-2}$ ). This means that energy transport in the plasma core can now, for the first time, be related to a theory-based scaling, including its mass dependence. It also emphasizes that the large size of JET makes its data particularly valuable for separating core and edge effects in the global energy balance.

### (c) ITER demonstration pulses in D–T

During DTE1, the best ever fusion performance in an ITER-like H-mode was obtained in a 3.8 MA/3.8 T discharge that was maintained in steady state by regular type I ELMs. This resulted in the production of a fusion energy of 21.7 MJ, a ratio of the fusion energy produced to the input energy of 0.18 over 3.5 s (*ca.* 8 energy confinement times) and 4 MW of fusion power being maintained for *ca.* 4 s.

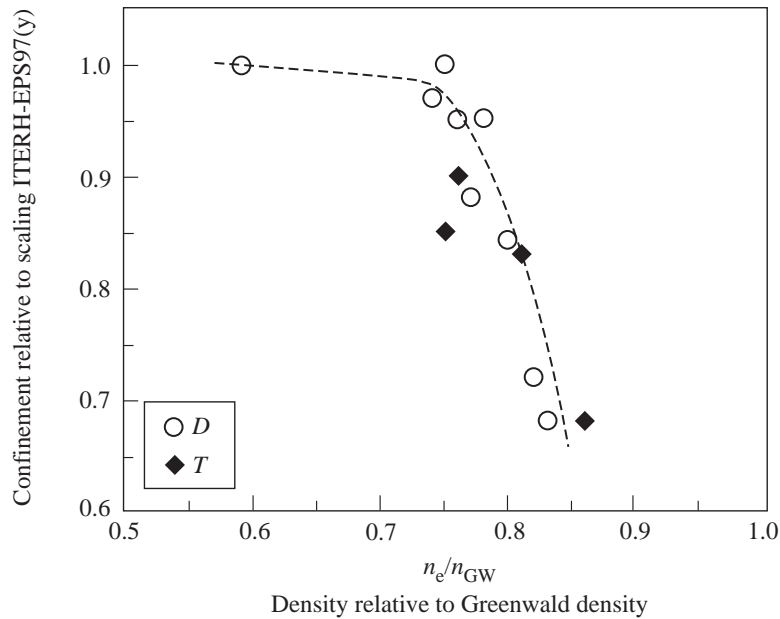


Figure 9. Energy confinement time relative to the ITERH-EPS97(y) scaling versus density relative to Greenwald density. Confinement starts to degrade above 75% of Greenwald density.

The normalized plasma pressure, being limited to  $\beta_N = 1.3$  by the available additional heating power (23 MW of combined NB (90%) and ICRF (10%) heating), was too low for these discharges to qualify as ITER demonstration pulses. However, at lower toroidal field and plasma current (e.g. at 2 MA/2 T), the normalized plasma pressure ( $\beta_N = 2.2$ ) and collisionality of an ignited ITER were closely matched on JET and the edge safety factor was also close to the ITER value ( $q_{95} = 3.2$ ). The characteristic signals of such a discharge in D–T are shown in figure 7; it forms the basis for a series of ‘wind tunnel’ experiments that preserves on JET all the relevant dimensionless parameters close to ITER values, except for the normalized plasma size,  $\rho^* = \rho_i/a$ .

The data from this series of experiments are shown, in figure 8, to scale close to gyro-Bohm, extrapolating to ignition in ITER. In fact, a gyro-Bohm extrapolation from these ITER demonstration pulses gives ignition at 1.8 GW (or  $Q = 5.8$  for a Bohm extrapolation) for ITER operating at 21 MA. The required density would, however, be 50% above the so-called Greenwald density limit, and confinement in JET and other tokamaks is degraded as this high density limit is approached (figure 9). During the 1998/99 campaign of JET experiments, the scaling of this density limit will be refined and the effect of deep fuelling using pellet injection rather than gas fuelling will be studied to determine any influence on confinement as higher densities are approached. Meanwhile, it has been possible to extend the ITER demonstration pulses to ITER operation at the higher plasma current of 24 MA (and correspondingly lower  $q_{95} = 2.76$ ). In this case, ignition is predicted at the 1.05 GW level for a gyro-Bohm extrapolation (or  $Q = 7.3$  for a Bohm extrapolation), but the required density is now lower and is close to the Greenwald density.

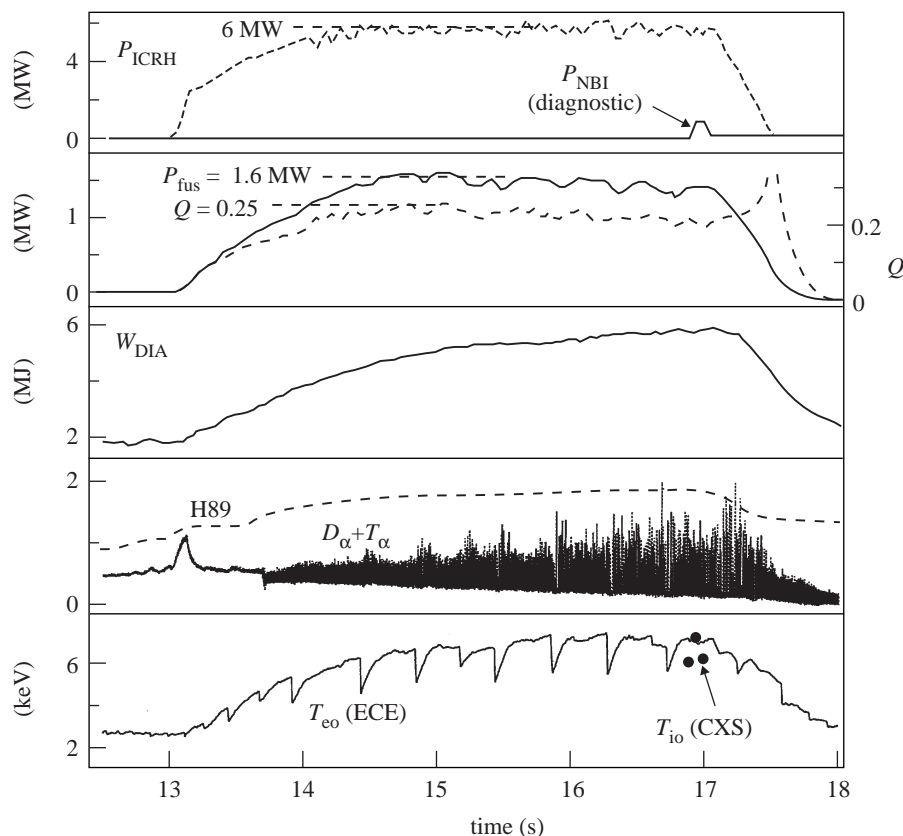


Figure 10. H-mode plasma in which 6 MW of D(T) ICRF heating power gave 1.66 MW of fusion power and  $Q = 0.22$  was obtained in quasi-steady-state. Pulse no. 43015; 3.7 MA/3.7 T.

#### 4. Ion cyclotron resonance frequency (ICRF) heating of D–T plasmas

ICRF heating is one of the main heating methods foreseen for ITER. During DTE1, the physics and performance of three ICRF schemes applicable to D–T operation ITER and a reactor were tested successfully (Start *et al.* 1998).

##### (a) Ion heating in deuterium and helium minority schemes

Deuterium minority heating, (D)T, at the fundamental resonance of deuterium ( $\omega_{cD}$ ) in tritium plasmas was demonstrated for the first time on JET (Start *et al.* 1998). The plasma density and the deuterium minority concentration (up to 20%) were optimized for maximum fusion power from reactions between suprathreshold deuterons and thermal tritons. For a pulse with 9% deuterium and 91% tritium, an ICRH heating power of 6 MW generated 1.66 MW of fusion power and the fusion  $Q$  of this steady-state discharge was maintained at 0.22 for the length of the RF heating pulse (three energy confinement times) (figure 10). Doppler broadening of the neutron spectrum (figure 11a) showed a deuteron energy of 125 keV, which was optimum for fusion reactions and close to the critical energy, resulting in strong bulk ion heating ( $T_{i0} = 7$  keV at  $n_{e0} = 5 \times 10^{19} \text{ m}^{-3}$ ) and high fusion efficiency.

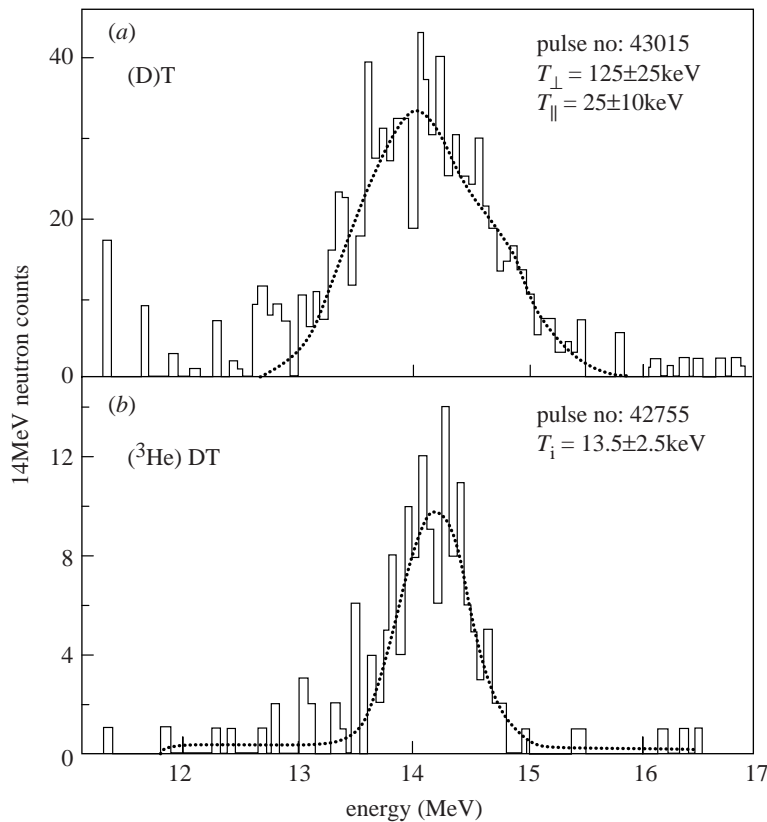


Figure 11. Doppler broadened neutron spectra for discharges with (a) deuterium and (b)  $^3\text{He}$  minority ICRF heating.

$^3\text{He}$  minority heating, ( $^3\text{He}$ )DT, at the fundamental resonance of  $^3\text{He}$  ( $\omega_{c^3\text{He}}$ ), in approximately 50:50 D:T plasmas with 5–10%  $^3\text{He}$ , also produced strong bulk ion heating. As seen from the neutron spectrum of figure 11b, the fusion reactions were thermal with central ion and electron temperatures of 13 and 12 keV, respectively. As discussed in § 4c, this scheme seems to be the most promising ICRF heating scheme for achieving ignition in ITER.

(b) *Electron heating in second harmonic tritium scheme*

Heating at the second harmonic of tritium ( $2\omega_{cT}$ ) in a 50:50 D:T plasma produced in JET energetic tritons well above the critical energy, resulting in mainly electron heating (ca. 90% of the power input). The fusion power was mainly from thermal reactions, but was typically a factor of four lower than with  $^3\text{He}$  minority heating under similar conditions. Second harmonic tritium and fundamental  $^3\text{He}$  minority ICRF heating are, of course, competing absorption mechanisms, since both resonances occur at the same position in the plasma.

The central ion and electron temperatures produced in these D–T experiments with the three ICRF heating methods are summarized in figure 12. The deuterium and  $^3\text{He}$  minority schemes generated strong bulk ion heating and ion temperatures

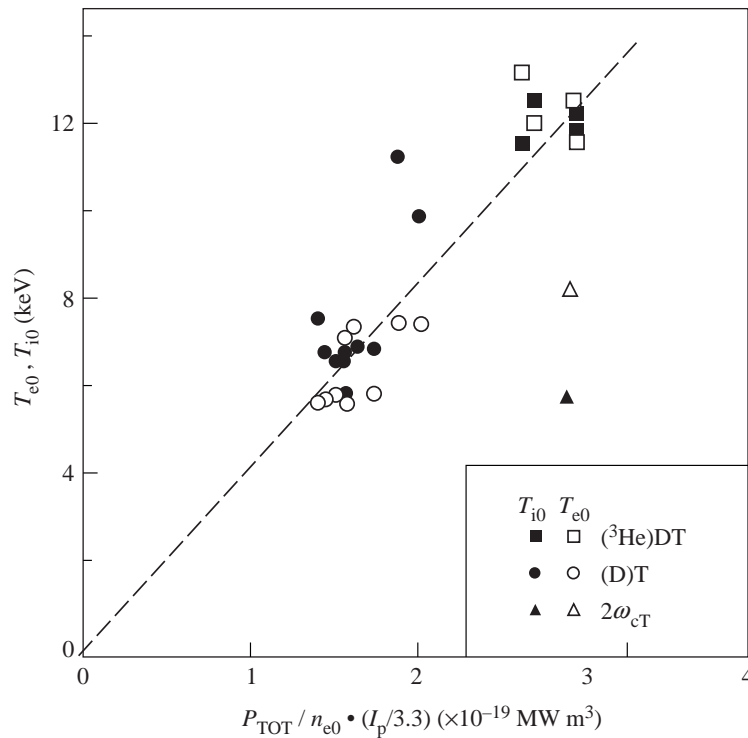


Figure 12. Central ion and electron temperature plotted against power per particle, corrected for values of plasma current different to 3.3 MA.

somewhat above the corresponding electron temperatures, whereas the second harmonic tritium ( $2\omega_{cT}$ ) scheme heated mainly the electrons. Figure 12 also shows that the mean central temperature,  $\frac{1}{2}(T_{e0} + T_{i0})$ , with  $2\omega_{cT}$  heating was considerably lower than with the minority schemes. This is a consequence of the loss of energetic tritons (with energies greater than 5 MeV) in JET at moderate plasma currents.

(c) Code calculations and predictions for ITER

Most of the results obtained in these ICRF heating experiments are in excellent agreement with PION code predictions, as exemplified by the comparison of measured and simulated neutron rates for a discharge with (D)T ICRF heating shown in figure 13. Such a high level of agreement inspires confidence in the use of these models for predicting ICRF heating in ITER. One result of these predictions is that the  $2\omega_{cT}$  scheme, which heats the electrons in JET, will give mainly ion heating in ITER where the power density per particle will be considerably lower, resulting in triton tail ions with lower energies. In addition, all fast ions will be confined in ITER, making heating at  $2\omega_{cT}$  an efficient bulk ion heating scheme.

The PION code has also been used to investigate the  $^3\text{He}$  minority scheme for ITER (Start *et al.* 1997). The results for a 2.5% concentration of  $^3\text{He}$  in a 50:50 D:T plasma and a power of 50 MW are shown in figure 14 in the form of contour plots of constant ion heating fraction in the  $n_{e0}$ ,  $T_{e0}$  space. For illustration, a ‘direct’

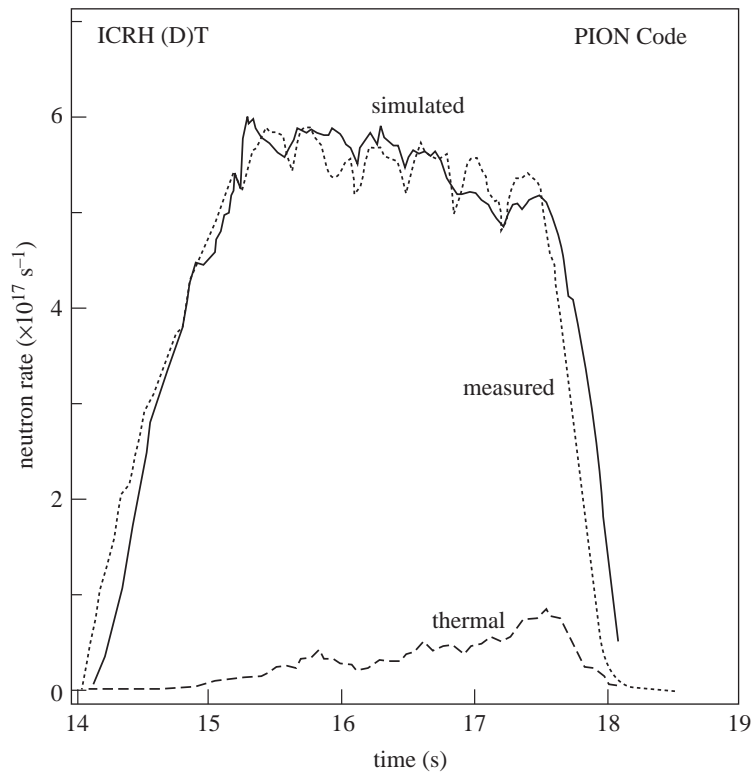


Figure 13. Comparison of measured and simulated (with PION code) neutron rates for a discharge with deuterium minority ICRF heating showing excellent agreement between the two. Pulse no. 43015.

route from the ohmic ( $T_{eo} = 5$  keV,  $n_{eo} = 3.5 \times 10^{19} \text{ m}^{-3}$ ) to the ignited phase ( $T_{eo} = 35$  keV,  $n_{eo} = 1 \times 10^{20} \text{ m}^{-3}$ ) is shown for which the ion heating fraction is larger than 70%, making it an excellent heating scheme for ITER. As heating progresses, the  $^3\text{He}$  concentration can be further reduced and the scenario changes to  $2\omega_{cT}$  ion heating.

## 5. D–T fusion performance and related physics

This section summarizes the most important results of DTE1 in the areas of fusion performance, Alfvénic instabilities and  $\alpha$ -particle confinement and heating (for a more detailed discussion, see Keilhacker *et al.* (1999)).

### (a) World records in fusion performance

In contrast to the steady-state ELMy H-mode discharge, which produced a record fusion energy (see § 3), the hot-ion ELMy-free H-mode is the traditional mode of highest, but transient, performance (JET Team 1997*b*) and, during DTE1, has led to records of fusion power and  $Q$ . In all, eight high-power ELM-free H-mode pulses were produced in D–T, five of which delivered more than 12 MW of fusion power. Figure 15 shows the pulse with the highest fusion power, 16.1 MW (a similar pulse

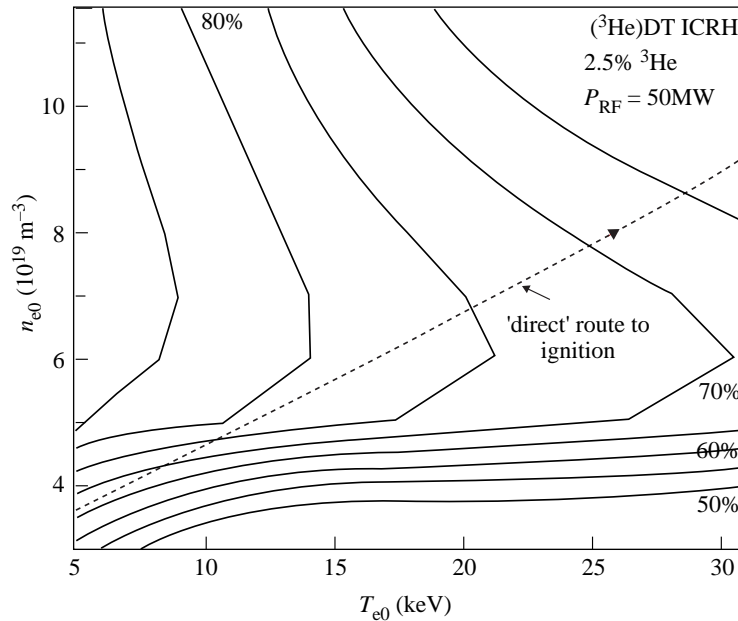


Figure 14. Contours of constant bulk ion heating fraction for ITER parameters and 2.5%  $^3\text{He}$  minority heating.

on the same day, about one hour earlier, produced 15.8 MW), which was obtained with 25.7 MW of additional heating using 22.3 MW of NB heating together with 3.1 MW of hydrogen minority ICRF heating. In common with the ELM-free H-mode discharges in deuterium, the stored energy (not shown), fusion power and electron density (not shown) rise monotonically with time. The ion temperature levels off around 28 keV, significantly higher than the electron temperature, which is about 14 keV. The ELM-free period is limited by MHD activity (as seen in the structure of the Balmer  $\alpha$ -signal): first an outer mode and then a giant ELM (Nave *et al.* 1997). Following detection of the giant ELM, the heating power is switched off to save neutrons. As shown in the lowest panel of figure 15, this pulse reaches a record fusion gain  $Q_{\text{in}} = P_{\text{fus}}/P_{\text{in}} = 0.62$  and a ratio of fusion power to total loss power  $Q_{\text{tot}} = P_{\text{fus}}/(P_{\text{loss}} - P_{\alpha}) = 0.95 \pm 0.17$  (Keilhacker *et al.* 1999), the value that  $Q_{\text{in}}$  would reach if a similar plasma could be obtained in steady state.

In addition, a thorough comparison of similar D–T and D–D discharges has validated the factor of 210 between D–D and D–T fusion power expected from the respective reaction-rate coefficients (Marcus *et al.* 1993). This is a very important confirmation that the expected fusion performance can be achieved in D–T.

Figure 16 summarizes the development of fusion power over the past six years in JET and TFTR. It encompasses the first ever high-fusion-power (1.7 MW) pulse with 11% tritium in JET in 1991 (JET Team 1992), the pulse with the highest fusion power (10.7 MW) (McGuire *et al.* 1997) from the 50:50 D D:T experiments on TFTR during the period 1993–1997, and finally the record pulses from the JET D–T experiments in 1997 (Keilhacker *et al.* 1999; Jacquinot *et al.* 1999): 16.1 MW, transiently, in an ELM-free H-mode, 8.2 MW in the optimized-shear mode of operation (see § 6), and 4 MW in a steady-state ELMy H-mode discharge.



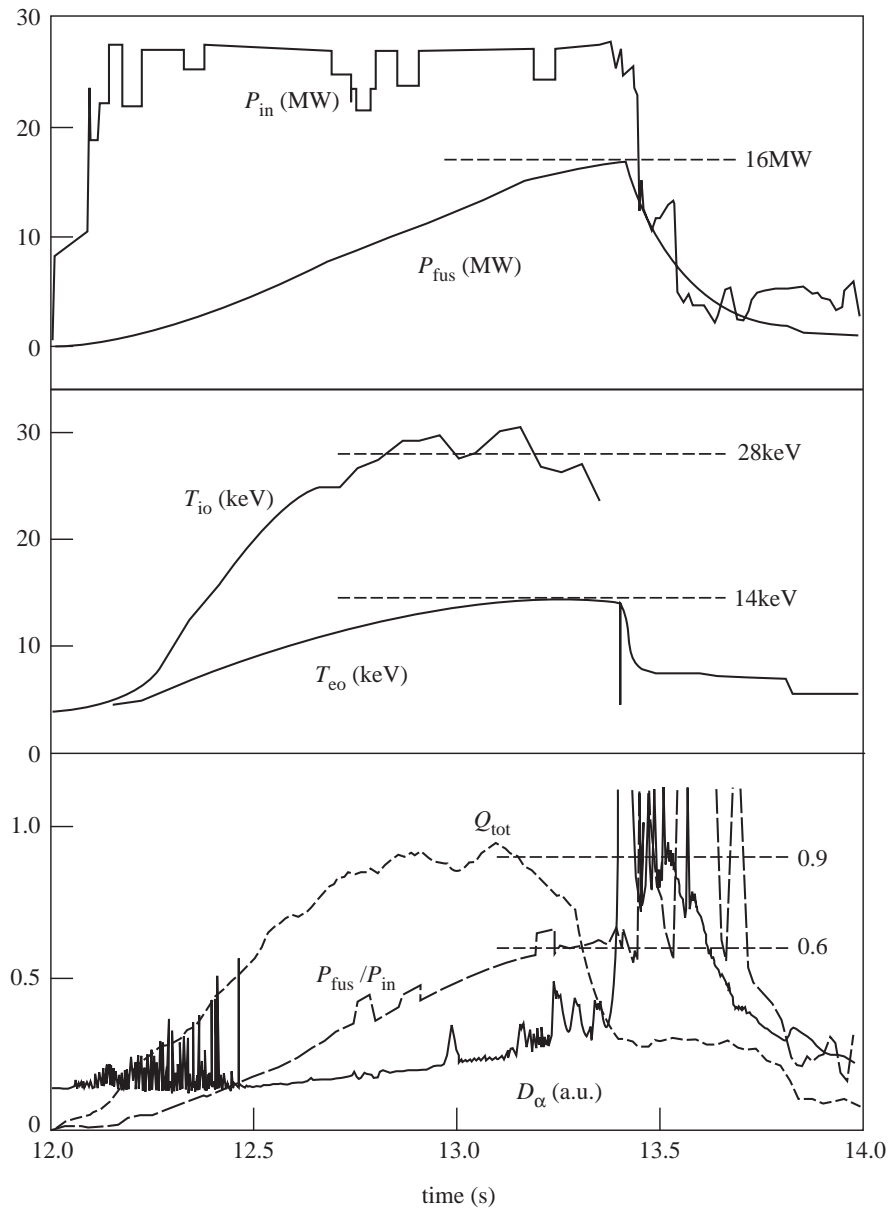


Figure 15. Various time traces for the highest fusion yield hot-ion H-mode discharge. From top to bottom: input and fusion power; central ion and electron temperature; ratios of fusion to loss power,  $Q_{\text{tot}}$ , and of fusion to input power  $Q_{\text{in}}$ ; and  $D_{\alpha}/T_{\alpha}$  intensity. Pulse no. 42976; 4.2 MA/3.6 T.

(b) *Alpha-particle driven Alfvénic instabilities*

Fast particles involved in plasma heating (e.g. fast ions from ICRF heating or NB heating,  $\alpha$ -particles) can resonate with Alfvén waves, leading to particle and energy losses and possible destructive interaction with vessel components. An important

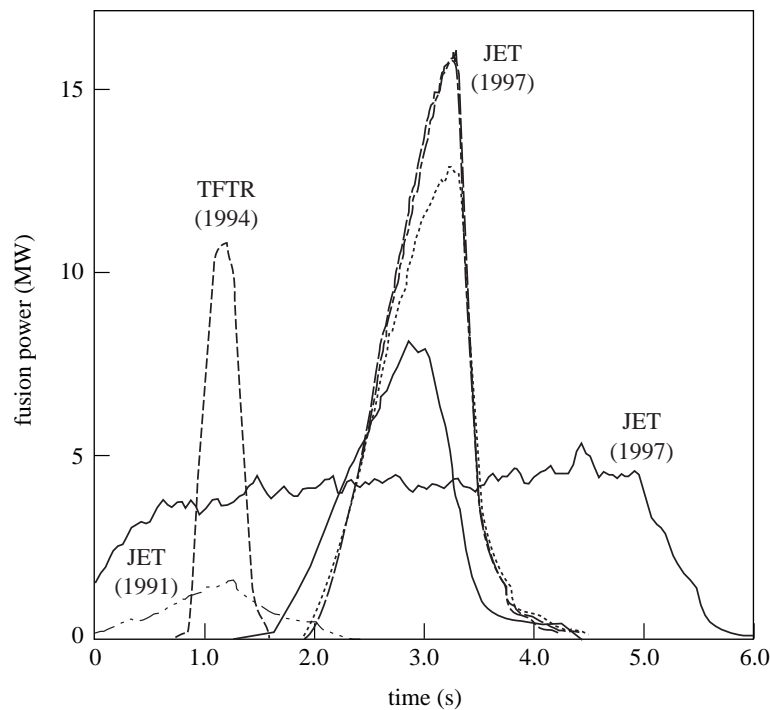


Figure 16. Fusion power development in JET (1991 and 1997) and TFTR (1994).

question in relation to high-performance fusion plasmas is, therefore, whether the  $\alpha$ -particles, while slowing down from their birth energy of 3.5 MeV, induce Alfvénic instabilities.

As can be seen from figure 17*b*, no  $\alpha$ -particle driven ‘toroidal Alfvén eigenmodes’ (TAEs) were excited in the record fusion power D–T discharges, even though TAEs have been observed under other circumstances in JET, e.g. with hydrogen minority ICRF heating in deuterium plasmas above an RF power of 5 MW (Fasoli *et al.* 1997), as seen from the magnetic fluctuation spectra shown in figure 17*a*. The absence of  $\alpha$ -particle driven instabilities in these high-performance discharges is in agreement with stability calculations that show that the normalized  $\alpha$ -particle pressure in these discharges is a factor of two below the instability threshold (Sharapov *et al.* 1999).

### (c) *Alpha-particle confinement and heating*

One of the most important objectives of the JET high-performance D–T experiments was an unambiguous demonstration of  $\alpha$ -particle heating, thus confirming the process by which ignition and self-sustained burn would occur in ITER and a reactor. Since JET plasmas with the highest fusion performance have about 3 MW of  $\alpha$ -particle heating compared to a total input power of about 25 MW, and the  $\alpha$ -particle heating is centrally peaked and couples mainly to the electrons, it should be observable, despite competition from other inputs to the electrons.

To separate the  $\alpha$ -particle heating from possible isotope effects on energy confinement, a series of specially designed pulses was carried out, in which the D–T mixture

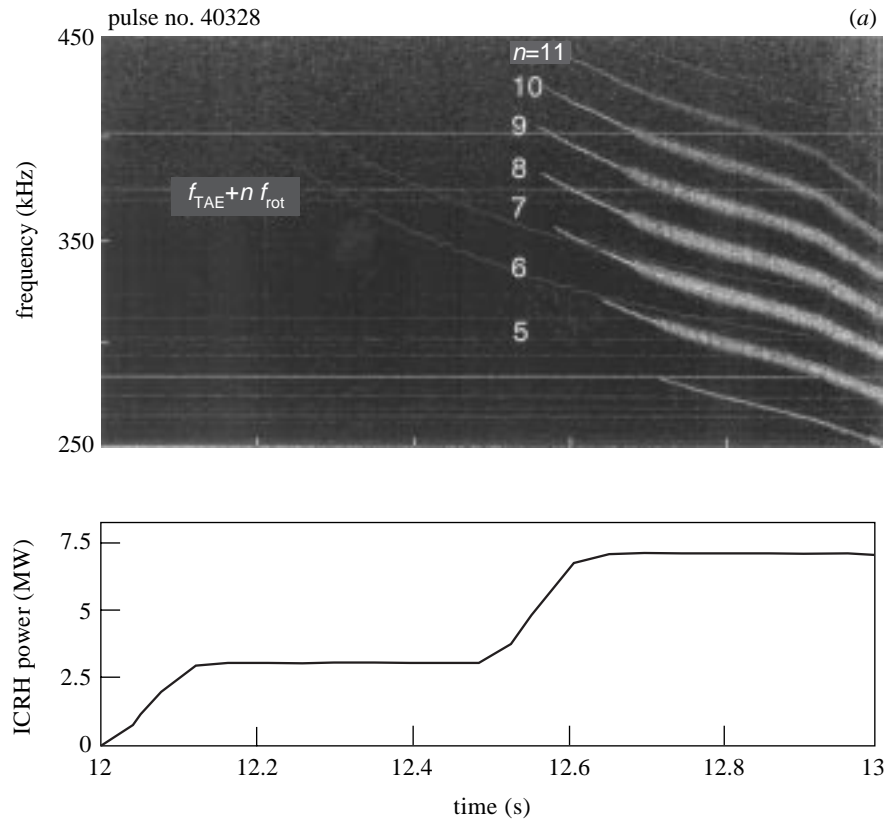


Figure 17. Magnetic fluctuation spectra showing (a) clear TAE activity above 5 MW of hydrogen minority ICRF heating but (b) no  $\alpha$ -particle driven TAEs in record fusion power discharge in D–T.

was varied from pure deuterium to almost pure tritium while all other parameters, including the external heating power (*ca.* 10.5 MW NB heating), were kept as constant as possible (Thomas *et al.* 1998). Comparing the pure deuterium and almost pure tritium ends of this scan demonstrated (lower panel in figure 18) that the global energy confinement time in ELM-free H-modes has no or only a very weak isotope dependence. The slight increase in confinement in the centre of the scan is due to the peaked  $\alpha$ -power source, which nearly doubled the power transferred to the electrons in the centre. The strong correlation between the maximum diamagnetic and thermal plasma energies and the optimum D–T mixture (upper panel in figure 18), is a clear demonstration of  $\alpha$ -particle heating. This is seen even more clearly in figure 19, which is a plot of the central electron temperature versus the calculated  $\alpha$ -particle heating power for the set of pulses in the D–T mixture scan. The highest electron temperature shows a clear correlation with the maximum  $\alpha$ -particle heating power and with the optimum D–T plasma mixture (40:60). A regression fit to the data gives a change in central electron temperature of  $1.3 \pm 0.23$  keV with 1.3 MW of  $\alpha$ -particle heating power.

These JET experiments are a clear demonstration of the self-heating of a D–T plasma by the  $\alpha$ -particles produced by fusion reactions. A comparison with ICRF

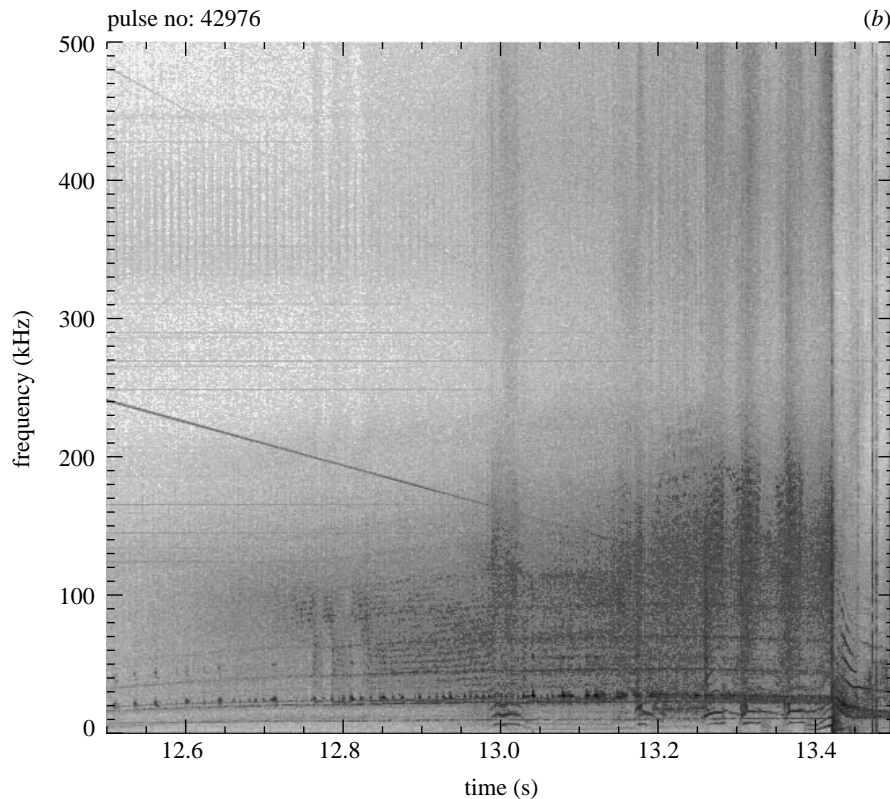


Figure 17. (Cont.)

heating of deuterium plasmas under similar conditions showed that the  $\alpha$ -particle heating was as effective as hydrogen minority ICRF heating (which, like the  $\alpha$ -particles, mainly heats the electrons). This is a strong indication that, in the absence of  $\alpha$ -particle driven TAE instabilities (see § 5*b*), the trapping and slowing down of the  $\alpha$ -particles and their heating effect are classical and that there are no unexpected effects that might prevent ignition in a larger device.

## 6. Advanced operating mode for ITER: optimized shear mode in D–T

The advanced tokamak concept proposes the use of profile control techniques to engineer high plasma confinement and to develop these conditions into steady state. This concept, if successful, would give ignition and sustained burn at lower plasma current, thereby reducing the size and cost of a reactor. JET has been particularly suited to such studies by virtue of its combination of heating schemes and its current drive capability. In fact, JET reported the first observations of such plasma behaviour in the ‘pellet-enhanced performance’ (PEP) mode of 1988 (JET Team 1988; Hugon *et al.* 1992). More recently, JET developed a particular optimized-shear scenario, in which pressure profiles are more peaked and D–D neutron yields are higher than in the ELM-free H-mode (JET Team 1997*c, d*).

*Phil. Trans. R. Soc. Lond. A* (1999)

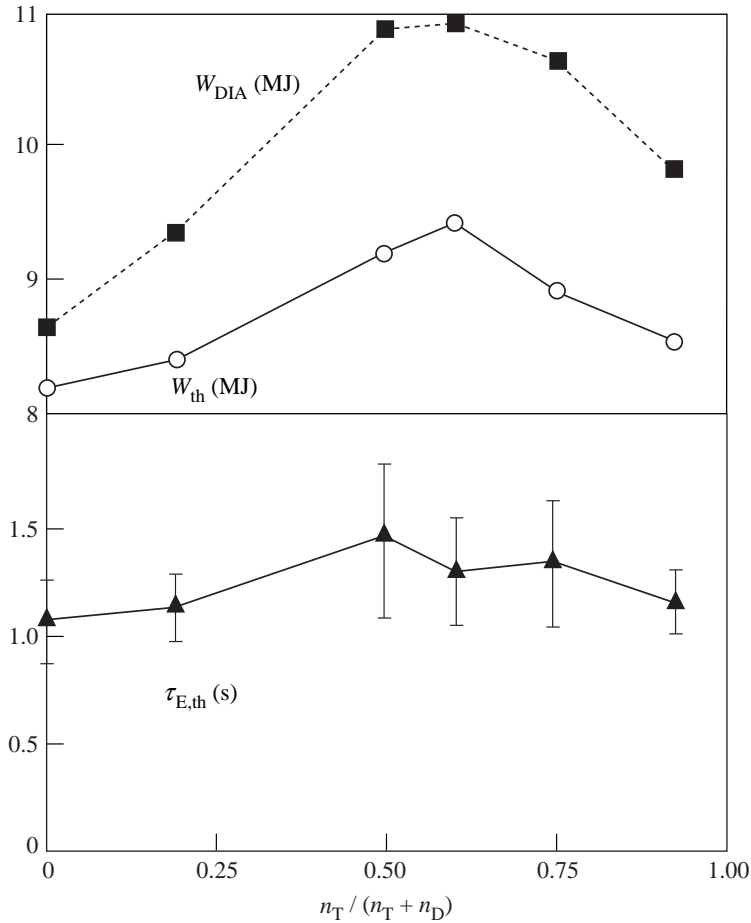


Figure 18. Diamagnetic and thermal plasma energy contents (top) and global energy confinement time (bottom) versus tritium concentrations. 3.8 MA/3.4 T/10.5 MW.

(a) *Formation of internal transport barriers*

A key element in these scenarios (JET Team 1997*c, d*; Kessel *et al.* 1994; Strait *et al.* 1995; Ushigusa *et al.* 1997) is the formation of ITBs (see figure 4), and these have now been established for the first time in D–T (Gormezano *et al.* 1998). Power and current profile controls are used to establish an ITB, to delay the transition to an H-mode phase, and to avoid a  $\beta$  limit disruption (JET Team 1997*c, d*). The scenario comprises the formation of a target plasma by pre-heating during a fast current ramp, using lower hybrid waves to assist breakdown and to provide some current drive, followed by ICRF pre-heating to slow current penetration. When the current profile is such that the volume within the  $q = 2$  surface is reasonably large ( $r/a \approx 0.3$ – $0.4$ ), the full heating power, typically 16–18 MW of NB heating together with 6 MW of ICRF heating, is applied (figure 20). In D–D, the highest fusion performance has been obtained when a clear H-mode transition was delayed for as long as possible by using low target density, strong divertor pumping and low triangularity and by maintaining the current ramp throughout the main heating phase. When an ITB

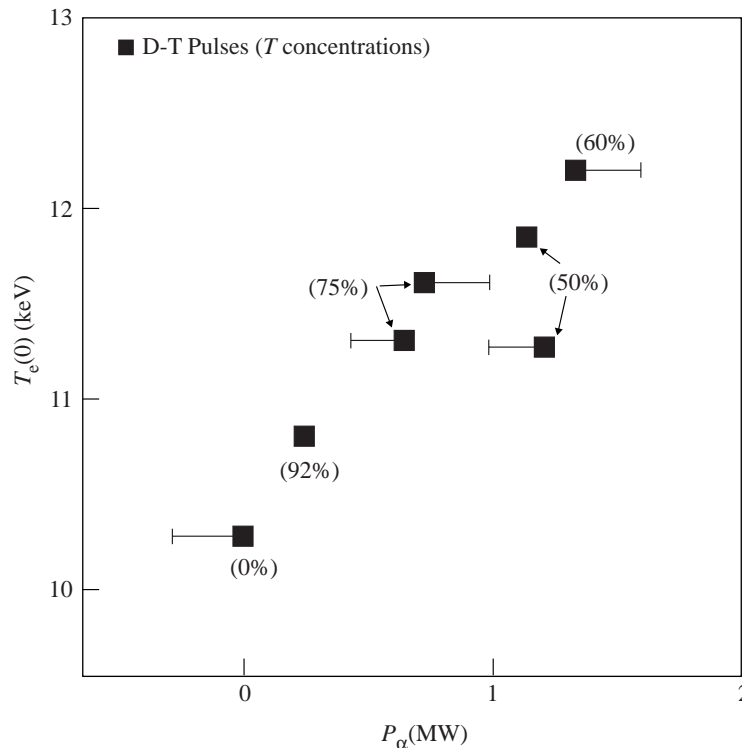


Figure 19. Central electron temperature versus  $\alpha$ -particle heating power. The bars indicate the variation in NB power compared to the 92% tritium reference pulse. The figures in brackets are the tritium concentrations.

is established, the resulting good core confinement maintains the plasma loss power below the level required to trigger an H-mode, thus preserving an L-mode edge.

In D–T, the scenario had to be modified, largely because of the lower H-mode threshold power (JET Team 1997a). However, after some scenario development, strong ITBs were established for the first time in D–T plasmas, and with a threshold heating power and current profiles not markedly different from those in D–D (Gormezano *et al.* 1998). In D–T, as in D–D, the foot of the steep gradient region was located just inside the  $q = 2$  surface and both moved outwards with time.

When an ITB forms, substantial increases in plasma density and temperature occur during the first second of high-power heating. As shown in figure 21, the temperature gradient can reach  $150 \text{ keV m}^{-1}$  and the pressure gradient  $1 \text{ MPa m}^{-1}$ . The input power is controlled by feedback on the neutron rate in order to avoid excessive pressure gradients that provoke MHD instabilities. As a result, the plasma can be maintained close to the ideal MHD stability limits for most of the heating pulse, as shown in figure 22 for optimized-shear discharges in D–D and in D–T (Huysmans *et al.* 1997). In both cases,  $\beta_N$  increases as the ITB moves outwards with time to *ca.*  $\frac{2}{3}$  of the plasma radius and the pressure profile becomes less peaked. Towards the end of the discharge, an H-mode forms, reducing further the peaking factor, moving the discharge away from the instability boundary but also leading to the subsequent termination of the discharge by disruption. The highest performance has

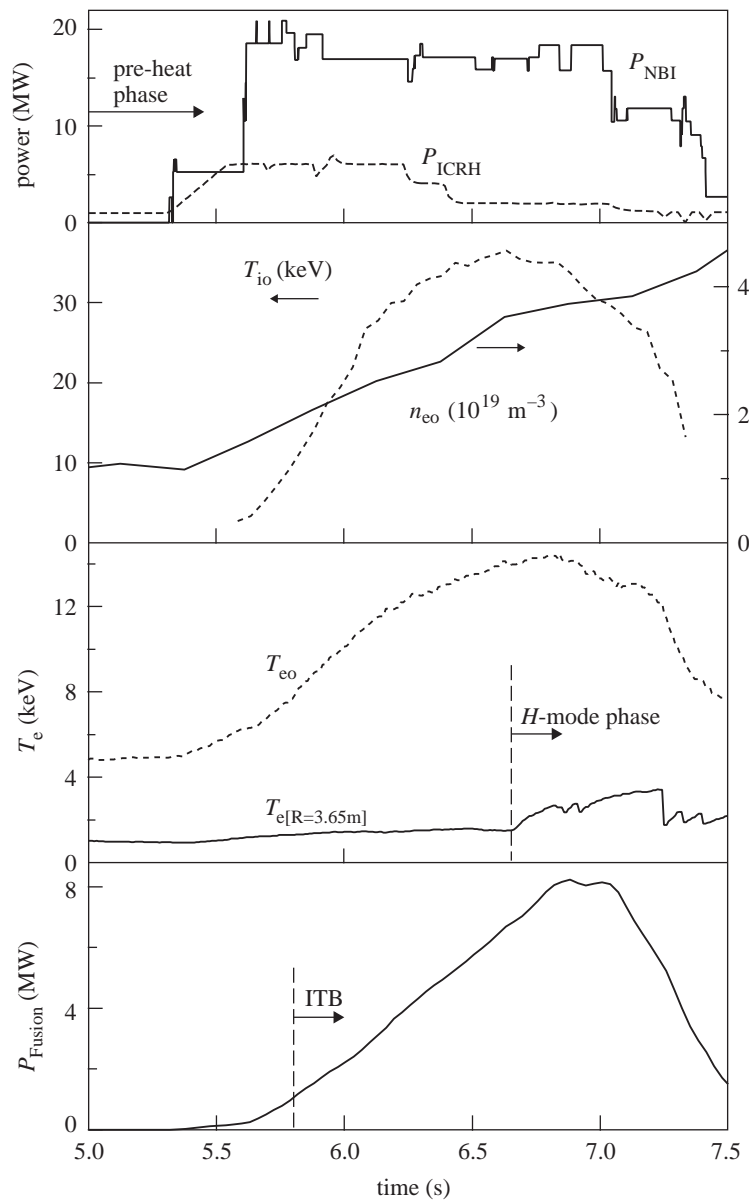


Figure 20. Various time traces for the optimized shear discharge with the highest fusion yield. From top to bottom: NB and ICRF input powers; central ion temperature and electron density; central and edge ( $R = 3.65$  m) electron temperatures; and fusion power. Pulse no. 42746; 3.3 MA/3.4 T.

been achieved with small or slightly reversed central shear and  $q(0)$  in the range 1.5–2.

This is confirmed by TRANSP simulations, which also show that more than half of the full plasma current at peak performance was driven non-inductively, with the

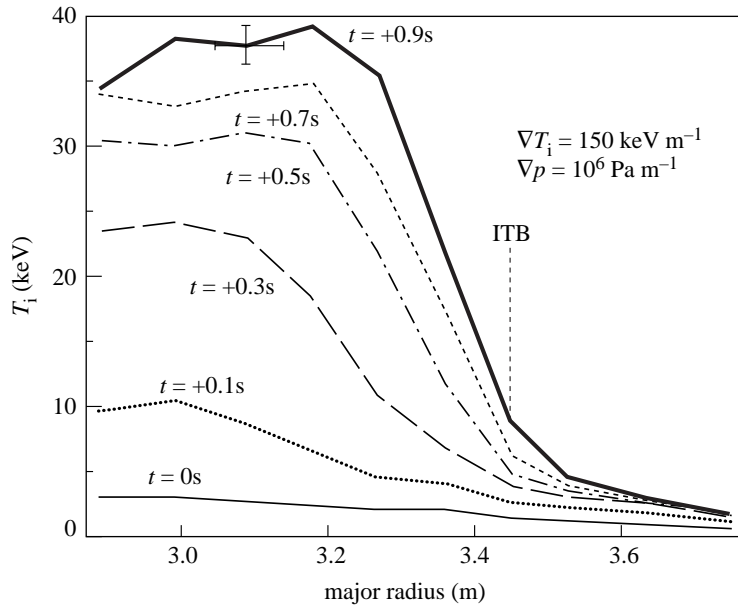


Figure 21. Ion temperature profiles at various times after the start of high-power heating in an optimized shear discharge showing the formation of an ITB. Pulse no. 42940 (D–T).

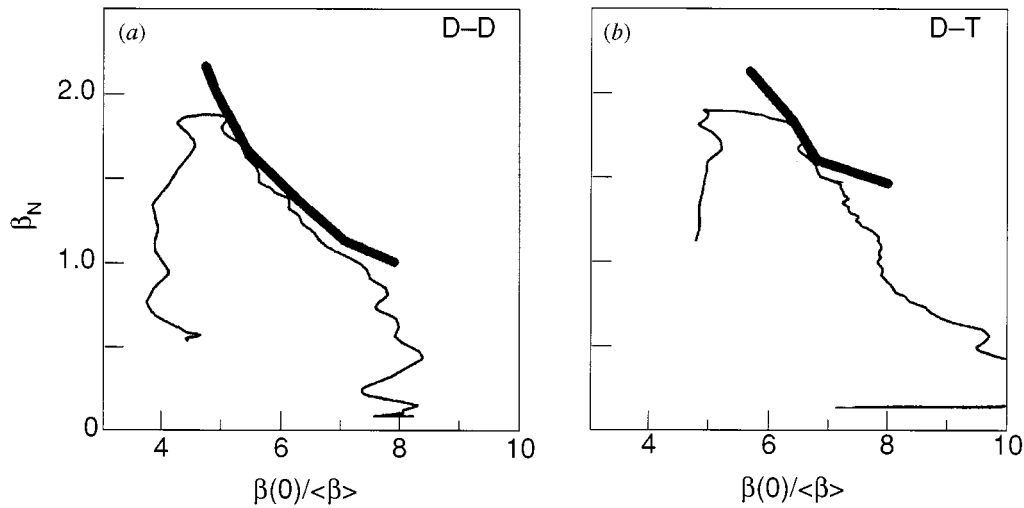


Figure 22. Stability diagrams for two optimized shear discharges: (a) in D–D (pulse no. 40847) and (b) in D–T (pulse no. 42746).

bootstrap and NB-driven currents being about equal and localized close to the centre. Furthermore, the TRANSP calculations show (Gormezano *et al.* 1998) that the ion thermal diffusivity can be very low and close to neoclassical (Hinton & Hazeltine 1976) values within the ITB (figure 23).

The neutron and time constraints on DTE1 did not allow these discharges to be optimized. Nevertheless, 8.2 MW of fusion power was produced (figure 20), even



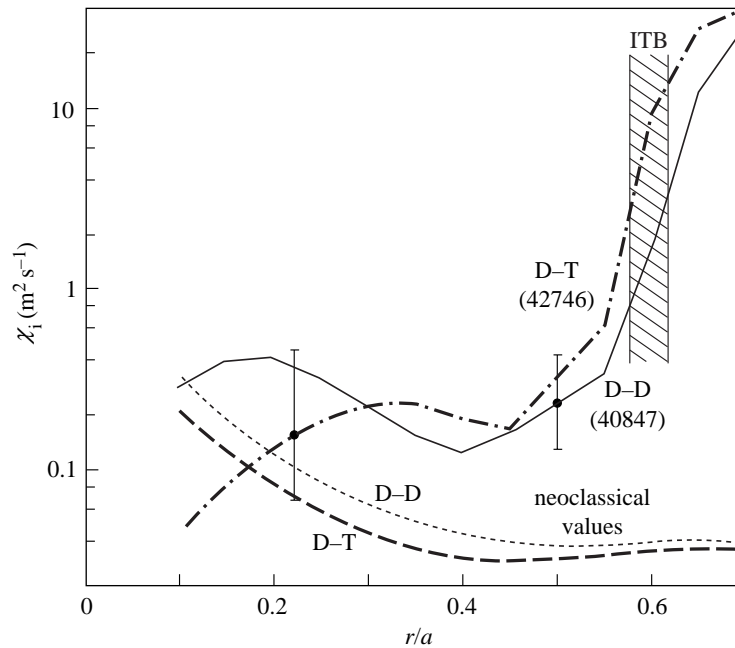


Figure 23. Ion thermal diffusivities versus normalized plasma radius for two optimized shear discharges in D–D and D–T and comparison with neoclassical values.

though the tritium concentration (*ca.* 30%) and central density ( $4 \times 10^{19} \text{ m}^{-3}$ ) were relatively low, and the ion temperature (*ca.* 40 keV) was too high for maximum fusion reactions.

(b) *Simultaneous internal and edge transport barriers and development towards steady state*

The highest fusion performance was normally obtained by prolonging the phase during which the plasma edge was L-mode (JET Team 1997*c, d*). A significant number of discharges, however, developed both an ITB and an ELMy H-mode edge (Keilhacker *et al.* 1999) as illustrated in figure 24, and still produced a substantial fusion yield. In the discharge shown in figure 24, an ITB is formed and the central ion temperature reaches 24 keV, while the edge ion temperature is about 3 keV, typical of an ELMy H-mode.

In this pulse, the fusion power increases from the start of the main heating phase until it reaches 6.8 MW, at which time the input power was reduced to economize on D–T neutrons. This increase in fusion yield is due to a continuous build-up of central density together with an increase in the tritium concentration. The stored plasma energy reaches 8.8 MJ for a total input power of 18.4 MW and a corresponding confinement enhancement factor  $H_{89} \approx 2.3$  relative to the ITER89-P scaling (Schissel *et al.* 1991). In this pulse, as in similar D–T and D–D pulses, the positions of the  $q = 2$  magnetic surface and the ITB change only slowly with time. This can be interpreted as a consequence of the generation of an edge bootstrap current. At 6.4 s, the input power was stepped down to limit the number of D–T neutrons produced; the subsequent collapse of the ITB triggers an ELM-free H-mode.

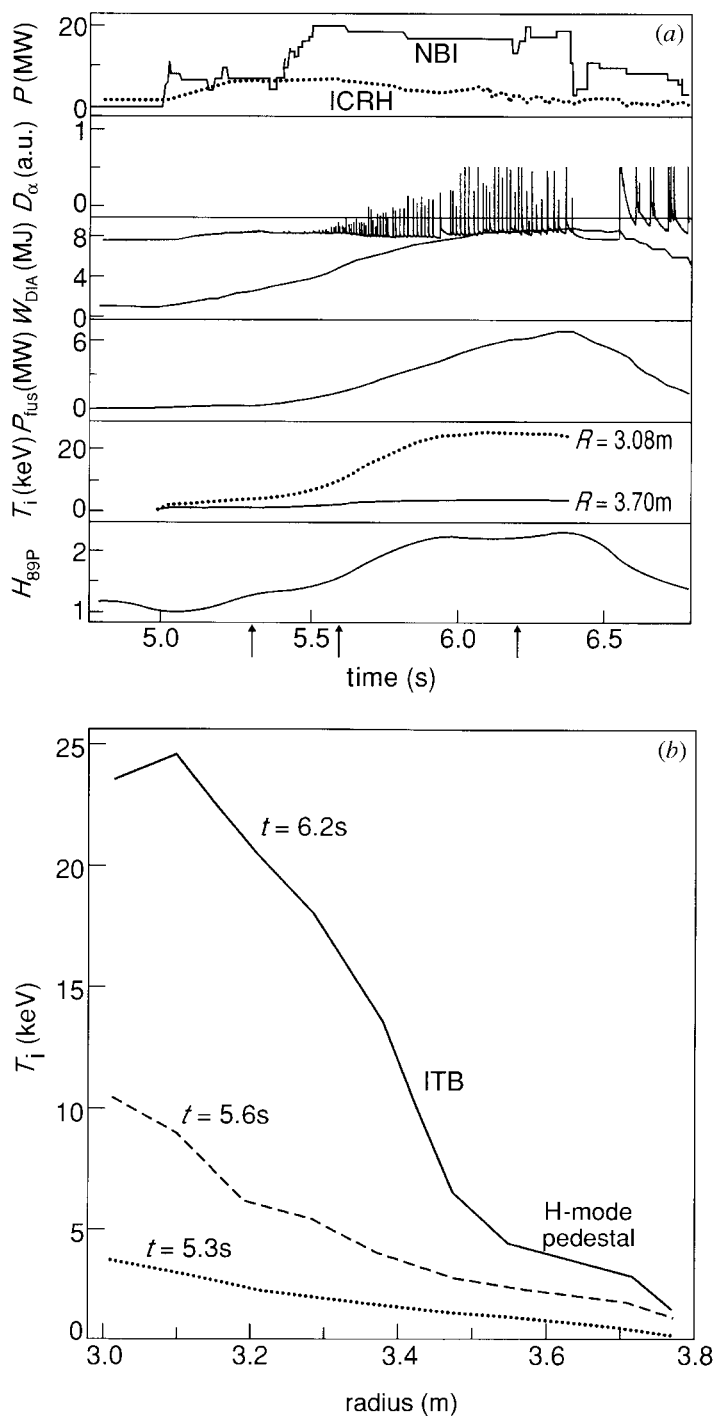


Figure 24. (a) Various time traces and (b) ion-temperature profiles for a pulse that develops an ITB simultaneously with an ELMy H-mode barrier (pulse no. 42733; 3 MA/3.45 T).

A comparison of the double-barrier (ITB plus ELMy H-mode) discharge, shown in figure 24, with a conventional ELMy H-mode discharge without an ITB in the same plasma configuration and with similar input power (22.5 MW), shows the advantage of the double-barrier plasma: the fusion triple product  $n_i(0)T_i(0)\tau_E$  reaches  $4.4 \times 10^{20} \text{ m}^{-3} \text{ keV s}$  compared to  $1.9 \times 10^{20} \text{ m}^{-3} \text{ keV s}$ , and the fusion  $Q$  is 0.4 compared to 0.2 (Söldner *et al.* 1999). In addition, ELMs are of much smaller amplitude in double-barrier discharges (the energy loss in a single ELM is typically a factor of ten smaller), which is of great significance because of the critically high peak-power loads on the divertor target plates in a standard ELMy H-mode ignited ITER scenario.

This route, which could not be explored further during DTE1 because of the imposed constraint on the number of D–T neutrons produced, shows significant promise for steady-state high fusion-yield D–T plasmas, but would require a technique for better control of the plasma edge and/or the current profile.

### (c) Projections to future JET operations

As indicated in § 6*a*, it was not possible to optimize the fusion performance of the optimized-shear discharges during DTE1 due to the constraints on time and neutron budget. Some code calculations were run, however, to determine what might be expected in future D–T operations on JET. These time-dependent transport code and MHD stability calculations, which have been calibrated against existing optimized-shear discharges in JET and Tore Supra, show that significant performance improvements are possible in JET (Keilhacker *et al.* 1998). The performance projections, in which the thermal fusion power is scaled from existing pulses as  $\beta_N^2$  and the non-thermal fusion power is scaled proportional to the NB heating power, predict, for operation with a magnetic field of 4 T, a fusion power of *ca.* 30 MW and a fusion gain  $Q_{\text{in}} = P_{\text{fus}}/P_{\text{in}} \geq 1$  with the existing heating and current drive systems, and even higher performance with modest upgrades.

## 7. Summary and conclusions

The recent D–T and ITER physics campaigns on JET have produced a wealth of unique and pertinent physics results, improving our theoretical understanding and allowing more accurate predictions for ITER.

The standard ITER operating mode (steady-state ELMy H-mode) has been well characterized empirically and a theoretical basis for energy confinement in the plasma core is within reach. The results of the dimensionless scaling ‘wind tunnel’ experiments extrapolate to ignition with ITER parameters.

Radio frequency heating of D–T plasmas is well understood and most effects are well simulated by theory. The results extrapolate to efficient bulk ion heating on the way to ignition in ITER.

Alpha-particle heating was clearly observed and is consistent with classical expectations, thus confirming the process by which ignition would occur in ITER and a reactor.

The advanced ITER operating mode (optimized shear) takes confinement to the most favourable theoretical expectations (i.e. ion heat conduction approaches neoclassical values), and the plasma pressure is limited in accordance with

theory. This improves the basis for performance optimization (high plasma pressure, long pulse) by profile control, which will be tested in subsequent JET operations.

With its unique combination of divertor configuration, heating and profile control systems and tritium capability, JET will remain, for many more years, the most valuable machine in support of ITER or any other ‘next step’ tokamak.

The author thanks all his colleagues at JET who have made these significant achievements possible and in particular M. L. Watkins, J. G. Cordey, C. Gormezano, P. J. Lomas, F. X. Söldner, D. F. Start and P. R. Thomas for their contributions to this paper, and B. E. Keen for his help with the editing.

### References

- Andrew, P. L. (and 21 others) 1999 *13th Conf. on Plasma Surface Interactions in Controlled Fusion Devices, San Diego, USA, 1998*. *J. Nucl. Mater.* (In the press.)
- Aymar, R., Chuyanov, V., Huguet, M., Parker, R., Shimomura, Y. and the ITER Joint Central Team and Home Teams 1997 In *Fusion energy 1996 (Proc. 16th Int. Conf. Montreal, Canada, 1996)*, vol. 1, p. 3. Vienna: IAEA.
- Fasoli, A. (and 11 others) 1997 *Plasma Phys. Control. Fusion* **39**, B287.
- Gibson, A. and the JET Team 1998 *Phys. Plasmas* **5**, 1839.
- Gormezano, C. (and 21 others) 1998 *Phys. Rev. Lett.* **80**, 5544.
- Hinton, F. L. & Hazeltine, R. D. 1976 *Rev. Mod. Phys.* **48**, 239.
- Hugon, M. (and 19 others) 1992 *Nucl. Fusion* **32**, 33.
- Huysmans, G. T. A. (and 13 others) 1997 In *24th Europ. Phys. Soc. Conf. on Controlled Fusion and Plasma Physics Berchtesgaden, Germany*, vol. 21A, Part 1, p. 21.
- ITER 1997a ITER Confinement Database and Modelling Expert Group (presented by T. Takizuka). In *Fusion energy 1996 (Proc. 16th Int. Conf. Montreal, Canada, 1996)*, vol. 2, p. 795. Vienna: IAEA.
- ITER 1997b ITER Confinement Database and Modelling Working Group (presented by J. G. Cordey). *Plasma Phys. Control. Fusion* **39**, B115.
- Jacquinot, J. (and 32 others) and the JET Team 1999 Overview of ITER physics deuterium–tritium experiments in JET. *Nucl. Fusion* **39**. (In the press.)
- JET Team 1988 The JET Team (presented by J. Jacquinot). *Plasma Phys. Control. Fusion* **30**, 1467.
- JET Team 1992 *Nucl. Fusion* **32**, 187.
- JET Team 1997a The JET Team (presented by M. Keilhacker). *Plasma Phys. Control. Fusion* **39**, B1.
- JET Team 1997b The JET Team (presented by P. J. Lomas). In *Fusion Energy 1996 (Proc. 16th Int. Conf. Montreal, Canada, 1996)*, vol. 1, p. 239. Vienna: IAEA.
- JET Team 1997c The JET Team (presented by C. Gormezano). In *Fusion energy 1996 (Proc. 16th Int. Conf. Montreal, Canada, 1996)*, vol. 1, p. 487. Vienna: IAEA.
- JET Team 1997d The JET Team (presented by F. X. Söldner). *Plasma Phys. Control. Fusion* **39**, B353.
- Keilhacker, M., Watkins, M. L. and the JET Team 1998 *Proc. 13th Conf. on Plasma Surface Interactions in Controlled Fusion Devices, San Diego, USA, 1998* (Invited Paper). *J. Nucl. Mater.* (In the press.)
- Keilhacker, M. (and 34 others) and the JET Team 1999 High fusion performance from deuterium–tritium plasmas in the JET tokamak. *Nucl. Fusion* **39**. (In the press.)
- Kessel, C., Manickam, J., Rewoldt, G. & Tang, W. M. 1994 *Phys. Rev. Lett.* **72**, 1212.
- Phil. Trans. R. Soc. Lond. A* (1999)

- McGuire, K. M. (and 142 others) 1997 In *Fusion energy 1996 (Proc. 16th Int. Conf. Montreal, Canada, 1996)*, vol. 1, p. 19. Vienna: IAEA.
- Marcus, F. B. (and 11 others) 1993 *Nucl. Fusion* **33**, 1325.
- Nave, M. F. F. (and 24 others) 1997 *Nucl. Fusion* **37**, 809.
- Schissel, D. P. (and 23 others) 1991 *Nucl. Fusion* **31**, 73.
- Sharapov, S. E., Borba, G., Fasoli, A., Kerner, W., Eriksson, L.-G., Heater, R. F., Huysmanns, G. R. & Mantsinen, M. J. 1999 Stability of alpha particle driven Alfvén eigenmodes in high performance JET D-T plasmas. *Nucl. Fusion* **39**. (In the press.)
- Söldner, F. X. *et al.* 1999 Approach to steady-state high performance in DD and DT with optimised shear in JET. *Nucl. Fusion* **39**. (In the press.)
- Start, D. F. H., Bergeaud, V., Eriksson, L.-G., Gayral, B., Gormezano, C. & Mantsinen, M. 1997 In *Europhysics Conference Abstracts (Proc. 24th EPS Conference on Controlled Fusion and Plasma Physics, Berchtesgaden, Germany, 1997)*, vol. 21A, Part 1, p. 141.
- Start, D. F. H. (and 31 others) 1998 *Phys. Rev. Lett.* **80**, 4681.
- Strait, E. J. (and 11 others) 1995 *Phys. Rev. Lett.* **75**, 4421.
- Thomas, P. R. (and 22 others) 1998 *Phys. Rev. Lett.* **80**, 5548.
- Ushigusa, K. and the JT-60 Team 1997 In *Fusion energy 1996 (Proc. 16th Int. Conf. Montreal, Canada, 1996)*, vol. 1, p. 37. Vienna: IAEA.

#### Discussion

R. J. HAWRYLUK (*Princeton Plasma Physics Laboratory, USA*). What was the value of  $\beta_N$  in the long pulse optimized-shear experiments? In the projections of  $\beta_N$  and fusion power,  $\beta_N > 2$ , which has been achieved to date. This implies that the current and pressure profiles have been ‘optimized’. Is the optimization achieved with the existing pressure and current profile techniques?

M. KEILHACKER. The maximum values for the normalized plasma pressure ( $\beta_N$ ) obtained in the JET long pulse optimized shear discharges were  $\beta_N = 1.5$  with ELMy H-mode edge and 1.8 with either L-mode or ELM-free H-mode edge. The reported projections were obtained from self-consistent transport-code modelling and MHD stability calculations. The improved performance shown by these projections results from a widening of the low-magnetic-shear core region, leading to broader and less peaked pressure profiles, which allow  $\beta_N = 2.6$  with existing heating and current drive systems.

R. S. PEASE (*West Ilsley, Newbury, UK*). It is very encouraging that Dr Keilhacker says that theoretical understanding of confinement is in sight; can he say more about the understanding of the high diffusion rates in the outer regions?

M. KEILHACKER. In some operating regimes (e.g. optimized shear mode, hot-ion H-mode), energy confinement in the plasma core and in the edge, respectively, is very good and in accord with theoretical expectations. However, the plasma between these two regions has significantly poorer confinement, typical of L-mode plasmas, and the theoretical basis is less clear. Future research will focus on further improving the understanding of transport in this intermediate region and reducing experimentally its influence.